ISSN 1075-7015, Geology of Ore Deposits, 2020, Vol. 62, No. 5, pp. 419–431. © Pleiades Publishing, Ltd., 2020.
Russian Text © The Author(s), 2020, published in Geologiya Rudnykh Mestorozhdenii, 2020, Vol. 62, No. 5, pp. 462–474.

# The Dudica Epithermal Cu–Au Deposit (Republic of North Macedonia)

**G. Tasev[a], D. Serafimovski[a], A. V. Volkov[b, *], B. Boev[a], T. Djordjevic[a], U. Kolitsch[c, d], and T. Serafimovski[a]**

[a] *Goce Delčev University, Štip, Republic of North Macedonia*
[b] *Institute of Geology of Ore Deposits, Petrography, Mineralogy, and Geochemistry, Russian Academy of Sciences, Moscow, 119017 Russia*
[c] *Institute of Mineralogy and Crystallography, University of Vienna, 1090 Vienna, Austria*
[d] *Department of Mineralogy and Petrography, Natural History Museum, 1010 Vienna, Austria*
**e-mail: alexander@igem.ru*

Received August 27, 2019; revised December 8, 2019; accepted March 14, 2020

**Abstract**—The Dudica deposit is located in the southern part of the Republic of North Macedonia (RNM), not far from the border with Greece in the Kozuf–Aridean volcanic region. The deposit is genetically associated with the Neogene igneous event (≥6 Ma, K/Ar), which is manifested at the intersection of northeast trending faults with the northwest trending Vardar fault zone. The REE spectrum of volcanic rocks here is characterized by a weak negative Eu anomaly and enrichment in light REE (LREE) relative to heavy REE (HREE). Mineralization is found in veins, veinlets, and dissemination; Cu concentration is around 0.5%; Au, up to 1 g/t. The principal ore minerals are chalcopyrite, bornite, enargite, covellite, chalcocite, and digenite; pyrite, galena, sphalerite, marcasite, and native gold are less frequent. The $\delta^{34}S$ isotope composition falls within a narrow interval of +1.00 to +2.50‰, indicative of the igneous origin. The data obtained suggest that the Dudica deposit belongs to the class of the high-sulfidation epithermal deposits.

*Keywords:* Republic of North Macedonia, Vardar zone, Dudica Au–Cu deposit, REE, mineral assemblage, sulfur isotopic composition, porphyry–epithermal system

**DOI:** 10.1134/S1075701520040054

## INTRODUCTION

The Dudica deposit is located within 2 km from the RNM–Greece border (Fig. 1). The deposit was periodically explored (1916–1917, 1940–1944, 1946–1948) but not mined except for native sulfur mining in small volumes. The deposit was covered by exploration operations in a considerable volume: several adits were driven, one of them being more than 400 m long, and more than 4 km core holes varying from 50 to 690 m in total depth were drilled. Exploration operations were based on the concept that the Dudica deposit is a volcanogenic massive sulfide (VMS) base metal deposit (similar to the Bor deposit in Serbia). Summaries of the Dudica deposit were published in Hiessleintner, 1945; Ivanov, 1965; and Jankovic, 1967.

Within the framework of this study, the authors undertook to update the geological characteristics of the Dudica region and the Dudica deposit, where Cu–Au mineralization is known. The geochemistry of the ore-bearing volcanic rocks of the Dudica deposit was studied, and their age determined for the first time. The sulfur isotopic compositions of the principal sulfide minerals were studied to establish the sources of the ore mineralization. The obtained data and comparison with similar deposits in the southern part of the Balkan Peninsula led us to the conclusion that the multimetal mineralization of the Dudica deposit belongs to the high-sulfidation epithermal class.

## MATERIALS AND METHODS

Rock samples for lithogeochemical analysis and isotopic dating were collected in 2015 from the ore stockpiles of exploratory adits and host rocks. The trace element compositions of the selected samples were determined using a combination of inductively coupled plasma atomic emission spectrometry (ICP-AES), mass spectrometry with inductively coupled plasma (ICP-MS), and instrumental neutron activation analysis (INAA) analytical techniques. The rock-forming oxides were analyzed by the ICP-AES method. The precision, as determined by the reproducibility of laboratory standards and duplicates, is within 5% for the major rock-forming oxides and 10% for minor and trace elements.

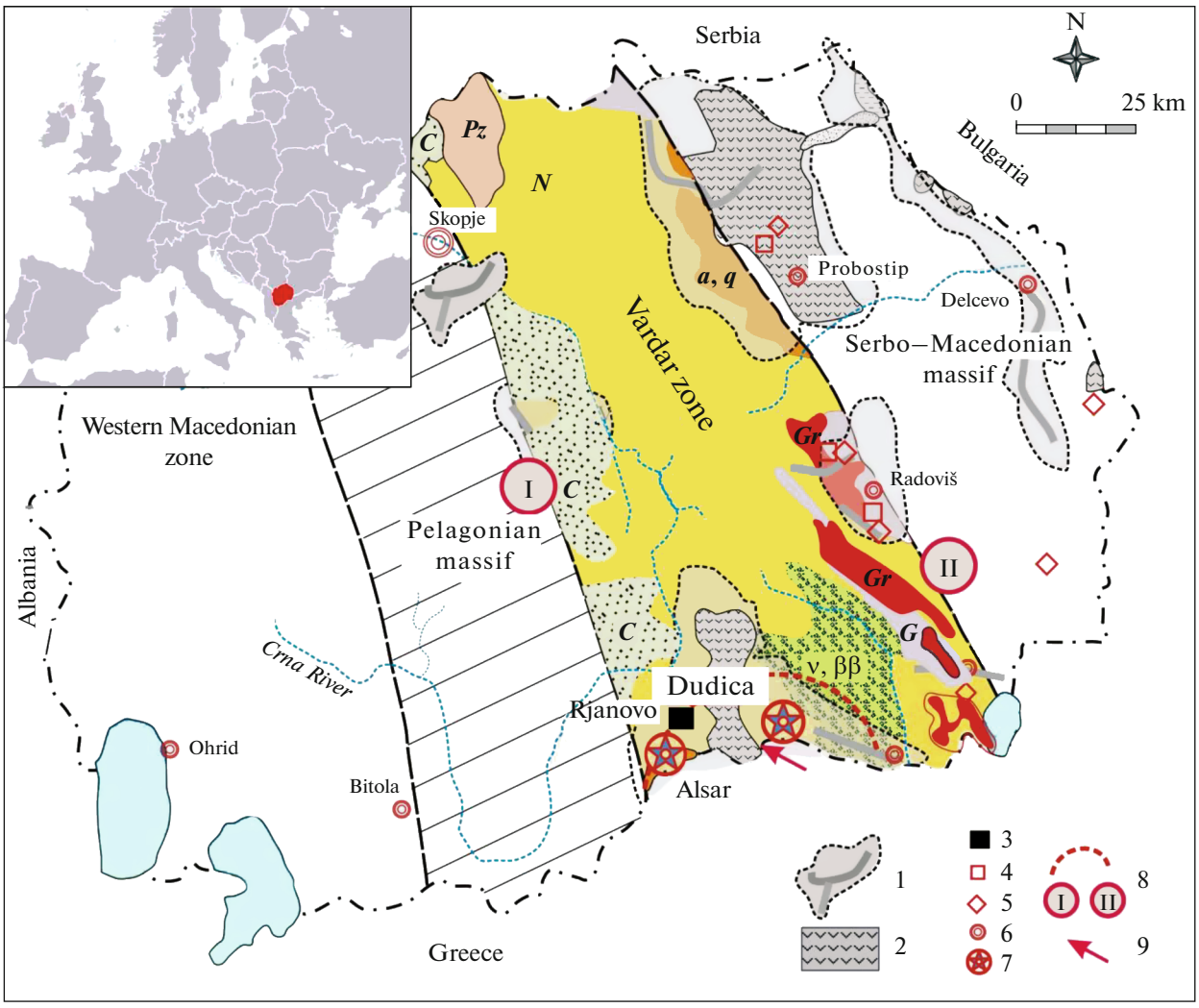


**Fig. 1.** Position of Dudica deposit in Vardar zone. (1) Potential ore districts; (2) Tertiary volcanic rocks; (3) Cu–Au deposit; (4) Cu deposit; (5) population center; (6) prospective ore deposits; (7) Kozuf volcanic zone; (8) regional lineaments; (9) sampling sites. N, Neogene, and Paleogene sedimentary strata; *a*, *q*, volcanics (Tertiary); *C*, Cretaceous sedimentary strata; ν, ββ, gabbro–diabases (Jurassic); *Gr*, granitoids (Jurassic); *Pz*, Paleozoic metamorphic rocks; *G*, gneisses (Precambrian).

The K–Ar ages of the rocks were determined at the laboratory of the Institute of Nuclear Research (ATOMKI) in Debrecen, Hungary. Potassium was measured by flame photometry with a Na buffer and a Li internal standard using a Sherwood M420 flame photometer. The precision and reproducibility of this method are within 2%. Argon was extracted in an ultrahigh vacuum system melting rock samples in molybdenum crucibles using radiofrequency induction heating. Argon isotope ratios were measured by diluting $^{38}Ar$ isotopes in compliance with the isotope dilution mass spectrometry method after the previous calibration using the atmospheric argon and international rock standards.

To determine $\delta^{34}S$ values for individual minerals, sulfide minerals were extracted from ore samples by handpicking under a binocular microscope. Pyrite, chalcopyrite, galena, and enargite samples crushed to 200 mesh in an agate mortar. Sulfur isotope analysis performed at the Acme Laboratory, Department of Geological Sciences, Queen's University, Kingston, Ontario, Canada.

## REGIONAL GEOLOGY AND METALLOGENY

The Dudica orefield is located on the western flank of the Vardar rift zone, at its contact with the Pelagonian crystalline massif (Fig. 1). It is within the Pliocene andesite–quartz latite volcanoplutonic complex in Aridea (Greece) and Kozuf in RNM. Only the northern Kozuf sector of this region was studied in detail (Ivanov, 1965; Jankovic et al., 1997; Bogojevski, 1998; Serafimovski and Tasev, 2013a; etc.).

The Kozuf–Aridean metallogenic zone of Pliocene mineralization occupies a specific position in the extreme south of the RNM, extending along the Greek border. The volcanic edifices and calc-alkaline subvolcanic intrusions are confined to northeast-trending neotectonic faults (Kochneva et al., 2006).

The Precambrian albitite gneisses with sporadic amphibolite lenses are the oldest rocks in the Kozuf–Aridea region and contain occasional marble blocks. Paleozoic schists, phyllites, metasandstones, argillaceous schists, and quartzites are of local extent. The Triassic deposits occupy a large part of the region. They are represented by two major facies, (1) marmorized limestones and dolomites and (2) argillites and sandstones with sporadic diabase and, sometimes, greenschist inclusions. The Late Cretaceous deposits are represented by Barremian–Albian conglomerates and Turonian limestones. The Upper Eocene strata consist of basal conglomerates overlain by flysch series (siltstones, mudstones, sandstones, and limestone beds). The Pliocene strata consist of conglomerates and muddy sandstones with calcareous mudstone interbeds. The volcano-sedimentary pyroclastic rocks and muddy sandstones occur in isolated Pliocene basins. The large part of the pre-existing Aridea volcanic crater is overlain by Pliocene deposits. The Quaternary deposits make up terraces.

The Tertiary igneous event started after the closure of the Mesozoic oceanic basin (Karamata, 1984). The closure resulted from the convergence of the Dinaride plate and the Carpathian–Balkan terrane with the Serbo–Macedonian massif and the subsequent collision of these continental segments (Dimitrijevic, 1974). The terminal phase of the Tertiary magmatism in the Vardar zone (including the Kozuf volcanic activity) during the Late Pliocene displays typical subduction-related characteristics (Boev and Yanev, 2001).

The characteristics of the Kozuf volcanic complex are discussed in detail by B. Boev (1988). Its composition represented by diverse types of andesites and quartz latites. The proportion of intrusive rock outcrops within the areal extent of this complex is insignificant because of a low erosion rate. The volcano-plutonic activity in the region lasted for 7 to 1.8 Ma.

The Late Jurassic subduction was accompanied by Middle and Late Cretaceous calc-alkaline magmatism (Boev and Jelenkovic, 2012). The post-subduction extensional tectonics generated intracontinental syn-orogenic faults, rift basins, and vast orogenic Tertiary magmatic belts of I-type plutonic and subvolcanic rocks. These partly differentiated giving rise to back-arc volcanism during the Miocene (Marchev et al., 2005).

*The Vardar reactivated fault system* consists of NW–SE trending (the oldest) and N–S trending faults (the youngest). The rocks of both the early and the main phases of volcanic activity (in the Dudica and Alsar areas) are located along these faults.

*The system of ring structures* manifested in the shapes of some topographic lows (visible in space images) and a topographic high in the Dudica area (Kochneva et al., 2006).

*The system of NE–SW to N–S trending faults* is younger than the Vardar system and characterized by recent seismic activity.

## GEOLOGICAL STRUCTURE OF THE DEPOSIT

The Dudica deposit occupies an area of several square kilometers. It is composed of Paleozoic schists, Upper Cretaceous limestones, and the rocks of the Late Tertiary volcanic complex (Fig. 2).

The Paleozoic complex comprises phyllites interbedded with sericite, chlorite, and epidote schists and marbles, as well as metamorphosed quartz porphyries and rhyolites.

The Paleozoic sequence in the southern part of the orefield is overlain by the Upper Cretaceous (Senonian) occasionally bituminous limestones. This limestone sequence (400–600 m in thickness) hosts the Ržanovo Fe–Ni deposit west of the Dudica orefield (Serafimovskii et al., 2013).

The Paleozoic and Upper Cretaceous strata in the central part of the Dudica orefield were intruded and/or overlain by igneous activity products during the Pliocene. These rocks are represented by dacite–andesite–quartz and rhyolite subvolcanic intrusions and northward-trending dike fields among a thick tuff sequence.

Faults are widespread in the Dudica orefield, especially in volcanic rocks. Sporadic brecciation zones are encountered in addition to faults and thin fracture systems. Some of these magmatic breccias are slightly mineralized. Several fault systems have been established thus far in the orefield. The SW–NE trending faults are predominant, but NW–SE trending faults are also present. Ore lodes are controlled mostly by SW–NE faults.

Volcanic rocks are propylitized, silicified, sericitized, carbonatized, and kaolinized. Limestones in the aureoles of the Pliocene subvolcanic intrusions underwent metasomatic silicification (up to the formation of large jasperoid bodies). Alunite-bearing secondary quartzite bodies and veins filled with porous–vuggy quartz are widespread in the orefield.

The ore-bearing zone in the Mircevica River valley is approximately 2 km long and 500–700 km wide. The lenticular elongate copper orebodies with minor swells are located along the Mircevica River channel (Figs. 2, 3). They are hosted by andesites and Cretaceous marmorized limestones, strongly altered by hydrothermal processes. The thickness of the mineralized contact zones is varying from 0.2 m to 20 m. The downdip ore continuity was not explored in detail.

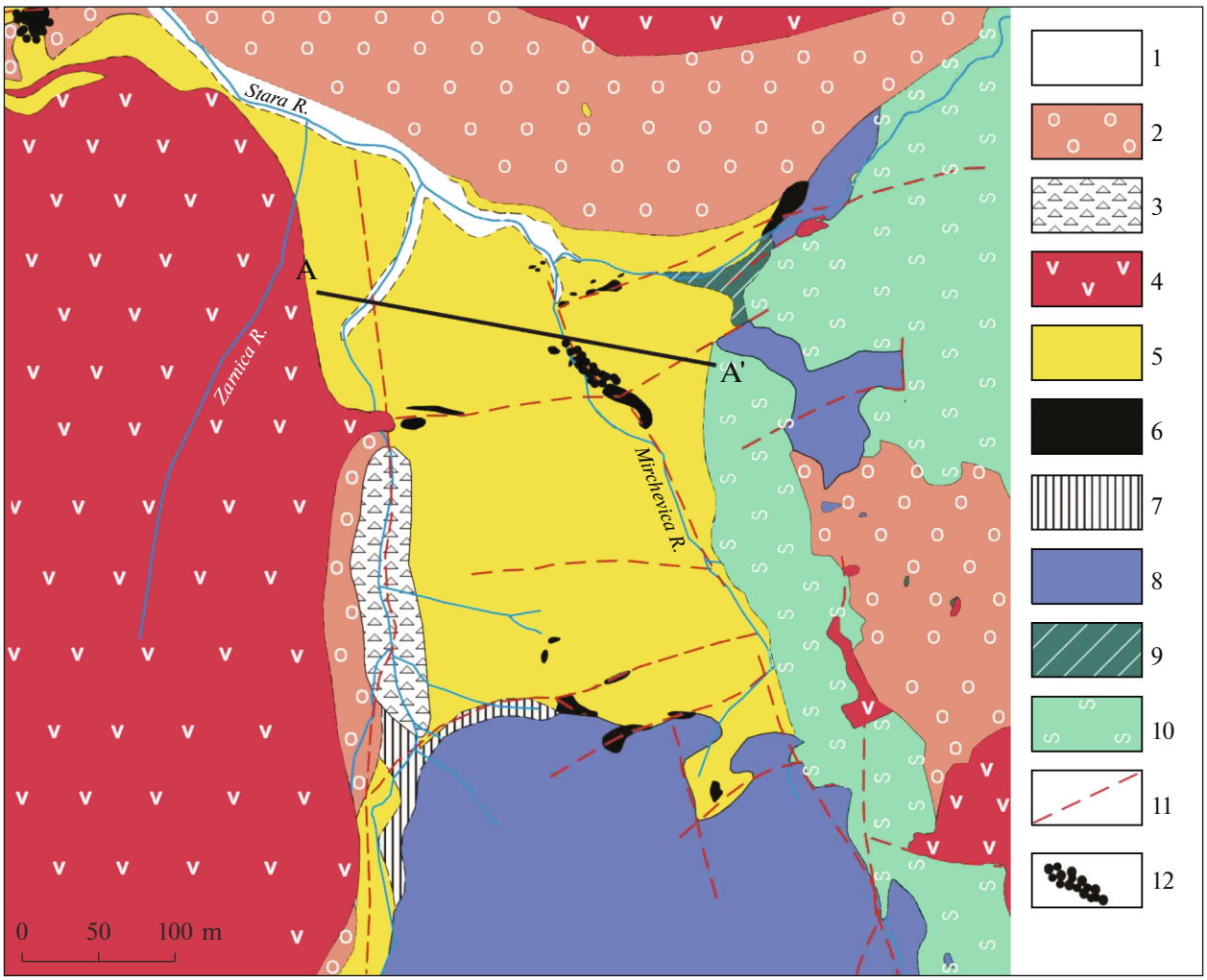


**Fig. 2.** Geological map of Dudica deposit (Ivanov, 1965; modified by Serafimovski and Tasev, 2013a). (1) Alluvium; (2) humus and slope wash; (3) andesite; (4) hydrothermally altered andesite; (5) secondary quartzite; (6) dacite, quartz porphyry; (7) marmorized limestone; (8) limestone; (9) sandstone; (10) Paleozoic schist; (11) faults; (12) mineralization.

The following *morphological types* of copper mineralization were established in the Dudica orefield:

1. *Hydrothermal veins* developed along faults, mostly in altered volcanic rocks (Fig. 3). Most veins have a thickness ranging from 0.1 to 0.3 m and up to 1.0 m in swells and a length ranging from several to 30 m, sometimes longer. Several enargite–pyrite–quartz veins with a thickness ranging from 0.1 to 1.0 m, which in some cases are subparallel to each other, were encountered in adit no. 6. The veins contain 3–5% Cu, up to 18 g/t Ag, and Au (mostly around 0.1 g/t; in places, 1.1 g/t).

2. *Veinlet systems* (in places as linear stockworks) that usually develop along fault zones up to several meters in width. Cu grade is usually 0.5–1.5%. Ag and Au grades were not determined.

3. *Disseminated mineralization* occurs mostly in schists and/or along their contacts with andesites. The stockwork-type disseminated (porphyry copper) mineralization was encountered by core drilling boreholes at deep horizons. The major ore minerals in this mineralization type are chalcopyrite and pyrite. Cu grade, according to drilling data, varies from 0.1 to 0.5%. Ag and Au grades were not determined.

The spatial distribution of a number of sulfide minerals at the Dudica deposit is of particular interest. It was studied from the surface (altitude 1800 m) down to 700 m levels (Jancovic et al., 1997). Illite, kaolinite, sericite, anhydrite, and pyrite were established in 1800–850 m. Enargite occurs in the interval of 1650–1230 m. The copper-bearing mineral group (bornite, covellite, chalcocite, and tetrahedrite) were emplaced in a relatively narrow depth interval of 1500–1220 m. Chalcopyrite, the main Cu-bearing mineral, was emplaced in 1400–850 m interval.

The jasperoids that were formed as a result of limestone and marble silicification were encountered in the southern part of the orefield. They can contain

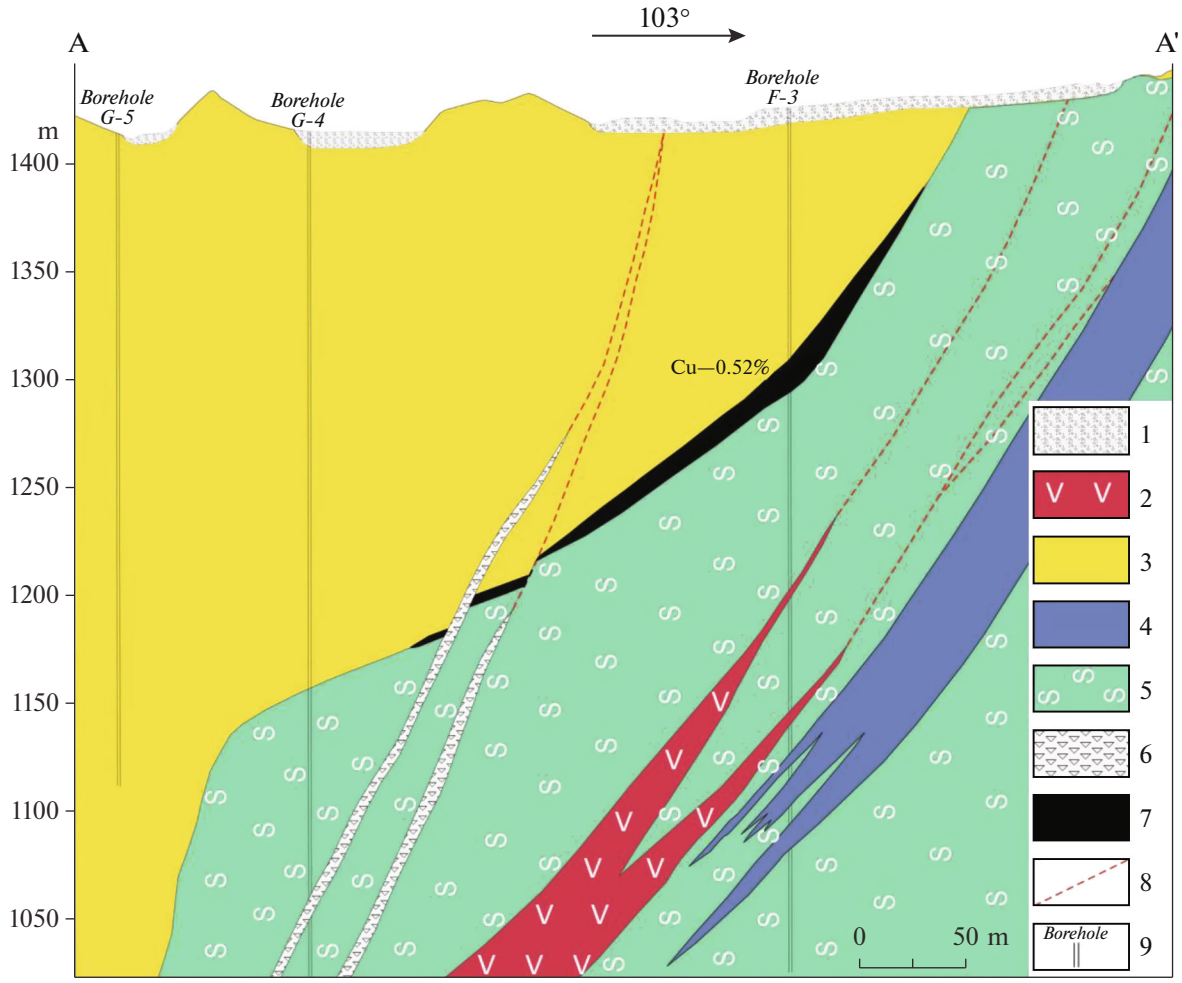


**Fig. 3.** Cross-section of Dudica deposit (modified after Ivanov, 1965). (1) Alluvium; (2) andesite; (3) hydrothermally altered andesite; (4) limestone; (5) Paleozoic schist; (6) crush zone; (7) orebody; (8) fault; (9) borehole.

carlin-type gold mineralization similar to the Alsar Deposit (Volkov et al., 2006). These jasperoids have not been analyzed for gold thus far. However, according to the data on two grab samples (one sample is from an outcrop), these rocks contain 7.2 and 13.4 g/t gold (Jankovic et al., 1997).

The lenticular bodies of native sulfur, a solfatara activity product, are frequently encountered along faults in the Dudica orefield. Around 20 t native sulfur was recovered during 1917 (Jankovic et al., 1997). Native sulfur occurrences in the orefield are of genetic rather than economic interest.

## GEOCHEMISTRY OF THE TERTIARY VOLCANIC ROCKS

The chemical compositions (major, trace, and rare earth element concentrations) of eight volcanic rock samples from the Dudica deposit are given in Table 1. They are consistent with the previously published data on the adjacent parts of the Kozuf area (Boev and Yanev, 2001; Boev and Jelenkovic, 2012). The photographs of the typical samples given in Fig. 4.

All samples can be characterized as high-potassium alkaline–shoshonite rocks: 58–65 wt % $SiO_2$; 3.55–4.77 wt % $K_2O$ (Table 1, Fig. 5; LeMaitre et al., 1989; Müller et al., 1992; Pearce, 1982; etc.). The rocks display insignificant $SiO_2$ content variations and stable concentrations of some major elements (wt %): 3.39–4.35 $Na_2O$; 2.95–5.48 CaO; and 0.47–2.45 MgO.

The volcanic rocks of the Dudica and adjacent igneous rock zones in the $SiO_2 – (K_2O+Na_2O)$ major element classification diagram (Middlemost, 1994) fall within the trachyandesite and trachydacite domain (Fig. 5a). The $K_2O–SiO_2$ plot (Fig. 5b) demonstrates that most samples fall within the field of high-potassium rocks and shoshonites, but one cannot exclude the possibility that the shift into the shoshonite field was caused by the metasomatic alteration of the analyzed rocks.

**Table 1.** Chemical composition of host rocks at Dudica deposit

| Element | D1S1 | D1S2 | D2S1 | D2S2 | Lat YB3 | Lat YB4 | Trdac YB5 | Trdac YB6 |
|---|---|---|---|---|---|---|---|---|
| $SiO_2$ (%) | 63.02 | 60.82 | 62.12 | 59.69 | 58.67 | 60.86 | 62.72 | 65.08 |
| $Al_2O_3$ (%) | 16.89 | 16.89 | 17.14 | 17.26 | 17.81 | 18.20 | 17.84 | 17.04 |
| $Fe_2O_3$(T) (%) | 4.34 | 5.1 | 4.54 | 6.02 | 5.51 | 4.64 | 4.12 | 3.39 |
| MnO (%) | 0.073 | 0.061 | 0.092 | 0.061 | 0.11 | 0.11 | 0.08 | 0.08 |
| MgO (%) | 1.66 | 2.45 | 1.76 | 2.4 | 1.50 | 1.11 | 0.79 | 0.47 |
| CaO (%) | 3.09 | 4.83 | 2.95 | 4.67 | 5.48 | 4.10 | 3.64 | 5.04 |
| $Na_2O$ (%) | 3.49 | 3.59 | 3.39 | 3.58 | 4.05 | 4.35 | 4.09 | 4.34 |
| $K_2O$ (%) | 3.62 | 3.58 | 3.61 | 3.55 | 4.71 | 4.75 | 4.77 | 3.84 |
| $TiO_2$ (%) | 0.473 | 0.648 | 0.487 | 0.651 | 0.71 | 0.52 | 0.50 | 0.43 |
| $P_2O_5$ (%) | 0.27 | 0.29 | 0.27 | 0.3 | 0.68 | 0.56 | 0.54 | 0.54 |
| LOI (%) | 2.58 | 2.21 | 2.67 | 2.06 | 0.78 | 0.80 | 0.90 | 0.47 |
| **Total (%)** | **99.51** | **100.5** | **99.03** | **100.2** | **100.01** | **100.00** | **99.99** | **100.72** |
| Sc (g/t) | 6 | 11 | 7 | 11 | 15 | 10 | 15 | 10 |
| Be (g/t) | 4 | 3 | 4 | 3 | – | – | – | – |
| V (g/t) | 78 | 108 | 79 | 106 | – | – | – | – |
| Cr (g/t) | 100 | 50 | 100 | 50 | 26 | 25 | 20 | 20 |
| Co (g/t) | 10 | 14 | 11 | 12 | 20 | 20 | 10 | 10 |
| Ni (g/t) | <20 | 20 | <20 | 20 | 30 | 20 | <20 | 20 |
| Cu (g/t) | 20 | 20 | 20 | 50 | | | | |
| Zn (g/t) | 60 | 60 | 50 | 50 | 80 | 100 | 20 | 20 |
| Ga (g/t) | 20 | 21 | 20 | 20 | – | – | – | – |
| As (g/t) | <5 | <5 | <5 | 9 | – | – | – | – |
| Rb (g/t) | 132 | 117 | 133 | 116 | 174 | 180 | 190 | 200 |
| Sr (g/t) | 994 | 1056 | 987 | 1070 | 1100 | 1170 | 1250 | 1250 |
| Y (g/t) | 10 | 15 | 11 | 15 | 34 | 34 | 26 | 23 |
| Zr (g/t) | 208 | 207 | 199 | 197 | 200 | 210 | 210 | 220 |
| Nb (g/t) | 9 | 9 | 8 | 10 | 7 | 6 | 4 | 1 |
| Sn (g/t) | 1 | 1 | 1 | 2 | – | – | – | – |
| Sb (g/t) | <0.5 | 1.1 | 0.6 | 1.6 | – | – | – | – |
| Cs (g/t) | 7.3 | 4.8 | 7.2 | 4.8 | 42 | 41 | 40 | 39 |
| Ba (g/t) | 1520 | 1539 | 1522 | 1544 | 1800 | 1760 | 1950 | 2100 |
| La (g/t) | 66.9 | 59.8 | 56.9 | 66.1 | 85 | 85 | 63 | 66 |
| Ce (g/t) | 130 | 114 | 115 | 122 | 145 | 157 | 125 | 115 |
| Pr (g/t) | 12.4 | 12.1 | 11.3 | 13 | 13.6 | 15.1 | 12.4 | 12.9 |
| Nd (g/t) | 42.7 | 44.5 | 39.8 | 47.6 | 54.8 | 56.9 | 41.3 | 51.2 |
| Sm (g/t) | 5.7 | 6.4 | 5.9 | 7 | 8.13 | 9.1 | 7.2 | 6.8 |
| Eu (g/t) | 1.43 | 1.68 | 1.41 | 1.78 | 2.0 | 1.9 | 1.42 | 1.38 |
| Gd (g/t) | 3.7 | 4.6 | 3.6 | 4.7 | 4.3 | 4.9 | 3.9 | 4.6 |
| Tb (g/t) | 0.4 | 0.6 | 0.5 | 0.6 | 0.75 | 0.78 | 0.7 | 0.7 |

**Table 1.** (Contd.)

| Element | D1S1 | D1S2 | D2S1 | D2S2 | Lat YB3 | Lat YB4 | Trdac YB5 | Trdac YB6 |
|---|---|---|---|---|---|---|---|---|
| Dy (g/t) | 2.3 | 3 | 2.4 | 3.2 | 3.3 | 3.8 | 2.9 | 3.3 |
| Ho (g/t) | 0.4 | 0.6 | 0.4 | 0.6 | 0.8 | 0.9 | 0.9 | 0.8 |
| Er (g/t) | 1.3 | 1.6 | 1.3 | 1.7 | 2.0 | 2.3 | 2.2 | 1.6 |
| Tm (g/t) | 0.2 | 0.23 | 0.21 | 0.26 | 0.33 | 0.36 | 0.34 | 0.28 |
| Yb (g/t) | 1.3 | 1.5 | 1.4 | 1.6 | 2.01 | 1.85 | 1.8 | 1.7 |
| Lu (g/t) | 0.22 | 0.25 | 0.21 | 0.25 | 0.30 | 0.28 | 0.34 | 0.38 |
| Hf (g/t) | 4.5 | 4.4 | 4.4 | 4.3 | 6 | 5 | 5 | 4 |
| Ta (g/t) | 0.9 | 0.8 | 0.9 | 0.8 | 0.8 | 0.8 | 0.7 | 0 |
| W (g/t) | 3 | 3 | 3 | 4 | 3 | 5 | 6 | 4 |
| Tl (g/t) | 0.8 | 0.7 | 0.8 | 0.7 | 1.1 | 1.5 | 4.1 | 3.3 |
| Pb (g/t) | 61 | 52 | 59 | 54 | 55 | 63 | 55 | 62 |
| Th (g/t) | 28.3 | 22.2 | 26.6 | 22.9 | 28 | 31 | 28 | 28 |
| U (g/t) | 8.2 | 7 | 8.1 | 6.9 | 8 | 9 | 6 | 8 |
| Sr/Y | 99.4 | 70.4 | 89.73 | 71.33 | 32.35 | 34.41 | 48.08 | 54.35 |
| La/Yb | 51.46 | 39.87 | 40.64 | 41.31 | 42.29 | 45.95 | 35.00 | 38.82 |

D1S1, D1S2, D2S1, and D2S2 are our latest samples; Lat YB3, Lat YB4, Trdac YB5, and Trdac YB6 are samples mentioned in (Boev and Yanev, 2001).

The rare earth elements (REE) in host rocks (Table 1) were normalized to the standard chondritic abundance values (Boynton, 1984). REE abundance and distribution trends in the latest samples from the Dudica area and samples from the Kozuf area (Boev and Yanev, 2001) are virtually similar (Fig. 6). The enrichment of samples in the light REE relative to the heavy REE indicate their origin from the same basaltic magma source within a subcontinental area. Almost all samples display a slightly negative Eu anomaly.

The geochronological (K/Ar) dating data for four rock samples from the Dudica deposit given in Table 2. The measured radiometric age values (5.0–6.5 Ma) overlap each other within the limits of the analytical error.

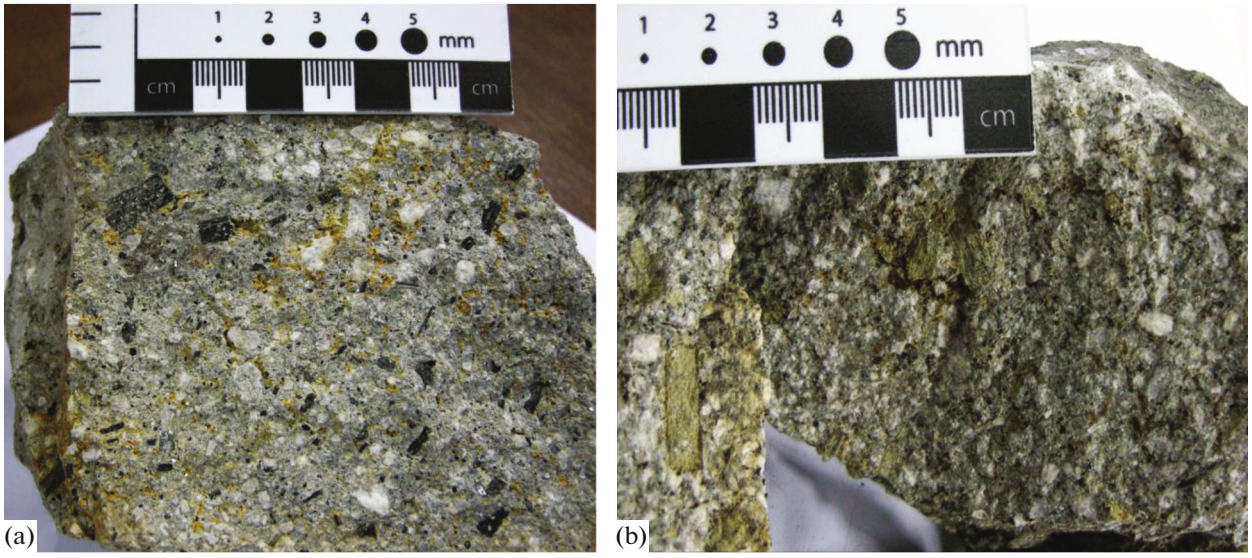


**Fig. 4.** Photographs of latest samples from Dudica area sent for chemical analysis: (a) sample D1S1; (b) sample D2S1.

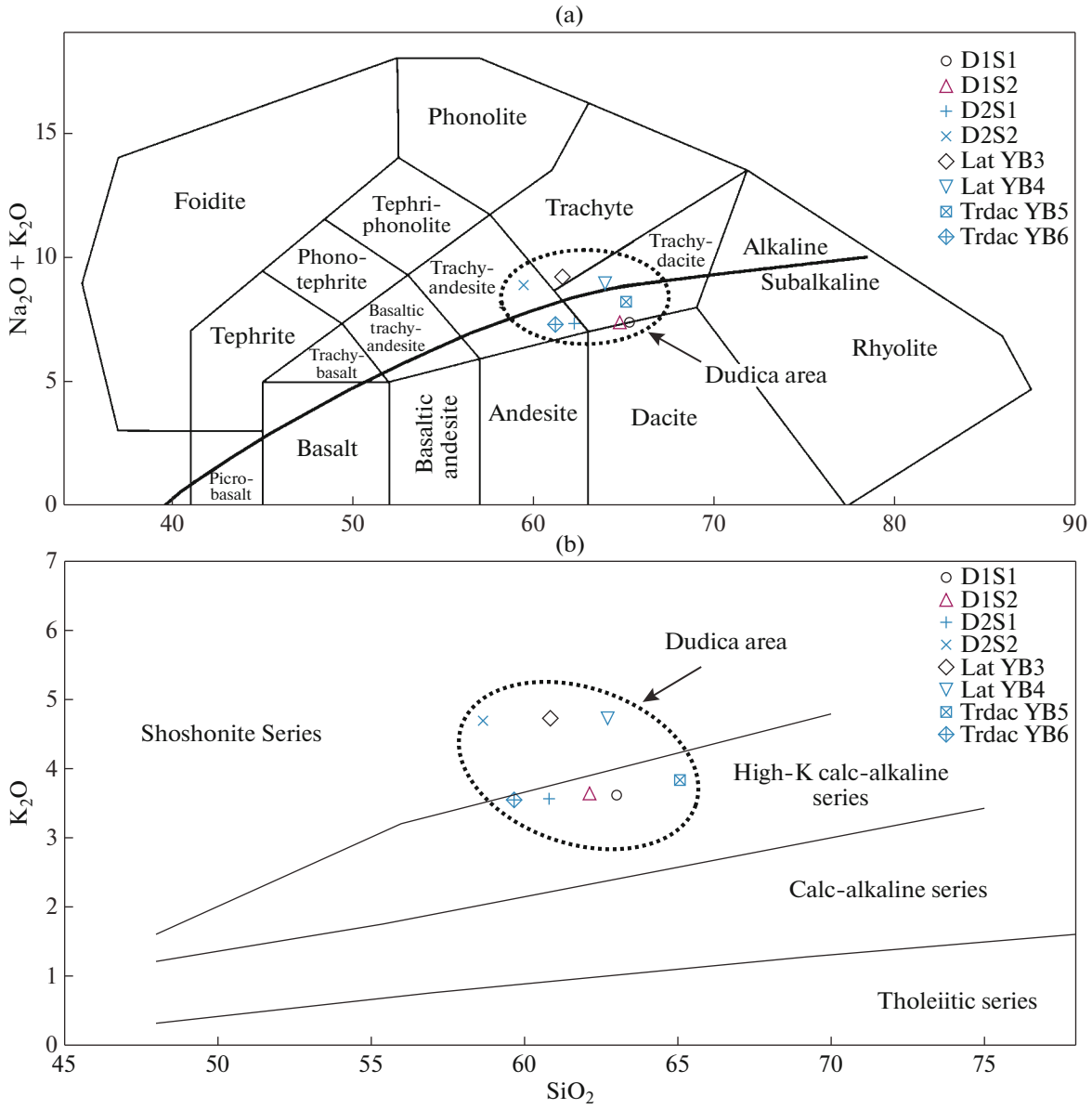


**Fig. 5.** Classification of igneous rocks in Dudica area (our analyses) and published data on Kozuf region (Lat YB3, Lat YB4, Trdac YB5, and Trdac YB6; Boev and Yanev, 2001).

## SULFUR ISOTOPIC COMPOSITION

To determine $\delta^{34}S$ values, four pyrite, three chalcopyrite, two galena, and two enargite monofractions were prepared and sent for analysis. The measured $\delta^{34}S$ values are given in Table 3. The $\delta^{34}S$ values vary from 1.0‰ to 2.3‰, average 1.80‰, for pyrite; from 1.5‰ to 2.1‰, average 1.70‰, for chalcopyrite; from 2.1‰ to 2.5‰, average 2.3‰, for galena; and from 1.8‰ to 2.4‰, average 2.1‰, for enargite. All of the analyzed sulfide minerals yielded $\delta^{34}S$ values vary from 1.0‰ to 2.5‰, average 1.9‰, with a variation range as narrow as 1.5‰.

## RESULTS, DISCUSSION, AND CONCLUSIONS

As mentioned above, the chondrite-normalized REE abundance values displayed normal differentiation with a very weak negative Eu anomaly (Fig. 6). The absence of significant Eu anomalies is probably due to the high degree of magmatic oxidation (Hanson, 1980; Carmichael and Ghiorso, 1990; Moore and Carmichael, 1998). An insignificant increase in Sr concentration with an increase in $SiO_2$ content in these samples rules out the possibility of significant plagioclase fractionation during the evolution of rocks in the Dudica area. Calculations based on the equations (see below) also yielded negative Eu and Ce

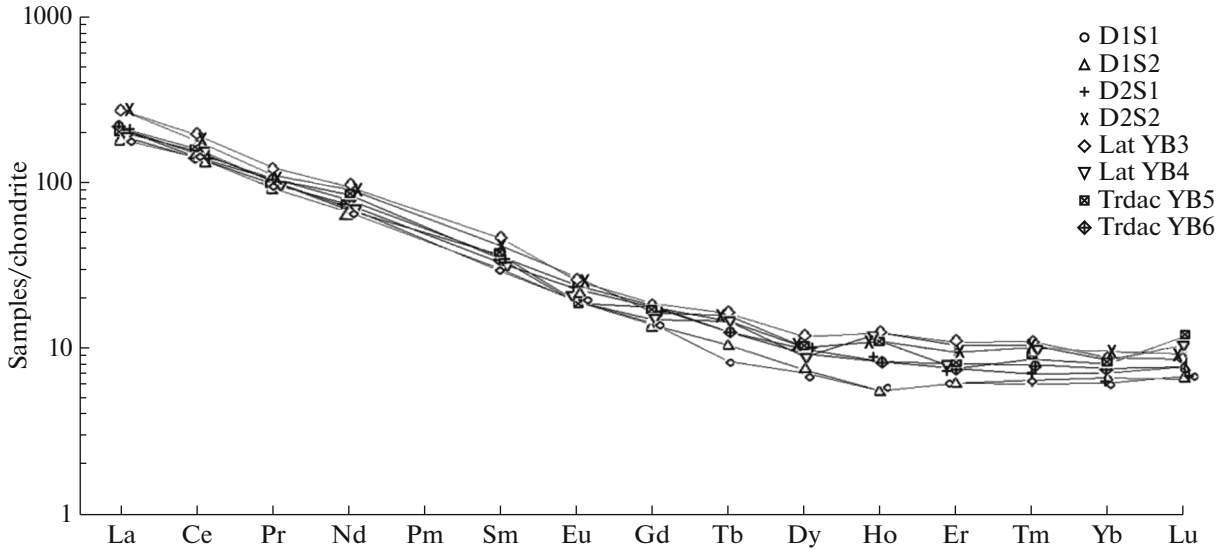


**Fig. 6.** Chondrite normalized REE diagrams of various rock samples from Dudica area (our analyses) and published data for Kozuf region (Boev and Yanev, 2001).

anomalies, except one value of Eu* = 1.034, which is slightly positive (sample 5-Lat YB3).

$$Eu^* = \frac{Eu_N}{\sqrt{Sm_N \cdot Cd_N}},$$

$$Ce^* = \frac{3Ce_N}{2La_N + Nd_N}.$$

Eu* values in the studied samples are varying from 0.7547 to 1.0343, average 0.9077, and Ce*, from 0.8354 to 0.9851, average 0.9151, indicating a mildly oxidizing ore-forming environment (Bau, 1991). The obtained data are similar to the data on other sectors of the Kozuf area (Jankovic et al., 1997; Boev and Yanev, 2001).

The Y–Rb, Ba–Rb, and Sr–Rb diagrams for these rocks (Figs. 7a–7c) demonstrate an increase in Rb and Y content with more or less constant Sr and Ba concentrations. These tendencies together, with the very weak Eu anomaly, attest to the limited participation of plagioclase in the differentiation process during latite and trachydacite formation. Clinopyroxene was probably the main fractionating mineral during the formation of these rocks (Boev and Yanev, 2001). According to the REE discrimination diagram (Fig. 7e), the Kozuf rocks demonstrate characteristics typical of subduction-related volcanic arcs.

Samples of host rocks (latite, trachydacite, andesite, and dolomite) from other sectors of the Kozuf region are characterized by close, subparallel REE distribution spectra (Jankovic et al., 1997; Boev and Yanev, 2001). The REE profiles of all samples (Fig. 6) demonstrate their enrichment in LREE and the presence of relatively flat HREE sections with slightly negative Eu anomalies, which is consistent with the hypothesis that HREE is less mobile than LREE and therefore remains predominantly in host rocks (McLennan, 1989). The enrichment in light REE (LREE) relative to heavy REE (HREE) is a feature in common for all samples from the Dudica deposit and Kozuf region (Jankovic et al., 1997; Boev and Yanev, 2001).

The high Sr/Y (32.35–99.40) and La/Yb (35.0–51.46) values (Fig. 8) may indicate high pressure and/or hydrous fractionation (Kolb et al., 2013). The enrichment in light REE (LREE) relative to the heavy (HREE) in the samples studied (Fig. 6), compared to the oceanic tholeiitic basalts, indicates the contribu-

**Table 2.** K/Ar geochronological analyses of host rocks at Dudica deposit

| Seq | Sample index | K, % | $^{40}$Ar rad (ccSTP/g ) | $^{40}$Ar rad (%) | K–Ar age ± 1 sigma |
|---|---|---|---|---|---|
| 1 | D1S1 | 3.484 | $8.1973 \times 10^{-7}$ | 18.9 | 6.04 ± 0.44 |
| 2 | D2S1 | 3.392 | $7.7663 \times 10^{-7}$ | 19.8 | 5.88 ± 0.41 |
| 3 | BBD1 L | 4.360 | $8.0230 \times 10^{-7}$ | 30.3 | 5.00 ± 0.40 |
| 4 | BBD2 LQL | 2.550 | $6.4080 \times 10^{-7}$ | 25.1 | 6.50 ± 0.41 |

Nos. 1–2, our samples; nos. 3–4, samples of B. Boev (Boev, 1988).

**Table 3.** $\delta^{34}S$ values of sulfides at Dudica deposit

| Sample index | Mineral | $\delta^{34}S$ ‰ |
|---|---|---|
| D1 | Pyrite | 1.0 |
| D2 | Pyrite | 2.3 |
| D4 | Pyrite | 2.0 |
| D5 | Chalcopyrite | 1.6 |
| D6 | Chalcopyrite | 2.1 |
| D7 | Chalcopyrite | 1.5 |
| D8 | Galena | 2.5 |
| D9 | Galena | 2.1 |
| D10 | Enargite | 1.8 |
| D11 | Enargite | 2.4 |

tion of crustal material during fractionation (Najime et al., 2012). Such a fractionation process is confirmed by $(La/Yb)_N$–$La_N$ and $(La/Sm)_N$–$Sm_N$ diagrams (Figs. 8a and b, respectively), as shown in (Chen et al., 2017).

The ΣREE values in rocks analyzed are relatively high (240.33–340.17 g/t); furthermore, ΣLREE values (230.31–325.00 g/t) are much higher than ΣHREE values (9.82–15.17 g/t), and this accounts for the high ΣLREE/ΣHREE values, ~18.958 to 26.388.

As mentioned earlier, the measured K–Ar radiometric ages of all samples (D1, D2, BBD1 L, and BBD2 LQL) overlap each other within the limits of analytical error and suggest Miocene to Pliocene age for the igneous activity in the Dudica area (Table 2). All samples are highly similar from the petrographic viewpoint (trachydacites).

Therefore, the K–Ar age can be considered as the minimum age (the real geological age can be somewhat older than the analytical one).

The measured ages demonstrate good agreement with the previous datings of 5.0–6.5 Ma for rocks in the Kozuf region (Boev, 1988) and 3.9 to 5.1 Ma, for individual minerals (biotite, feldspar) (Lipolt and Fuhrman, 1986; Boev and Jelenkovic, 2012).

As regards sulfur isotopic data, we compared $\delta^{34}S$ values of sulfide minerals with similar data within the Serbo–Macedonian metallogenic province (Tulare–Kiseljak, Plavica, Bucim, Borov Dol, and Skouries;

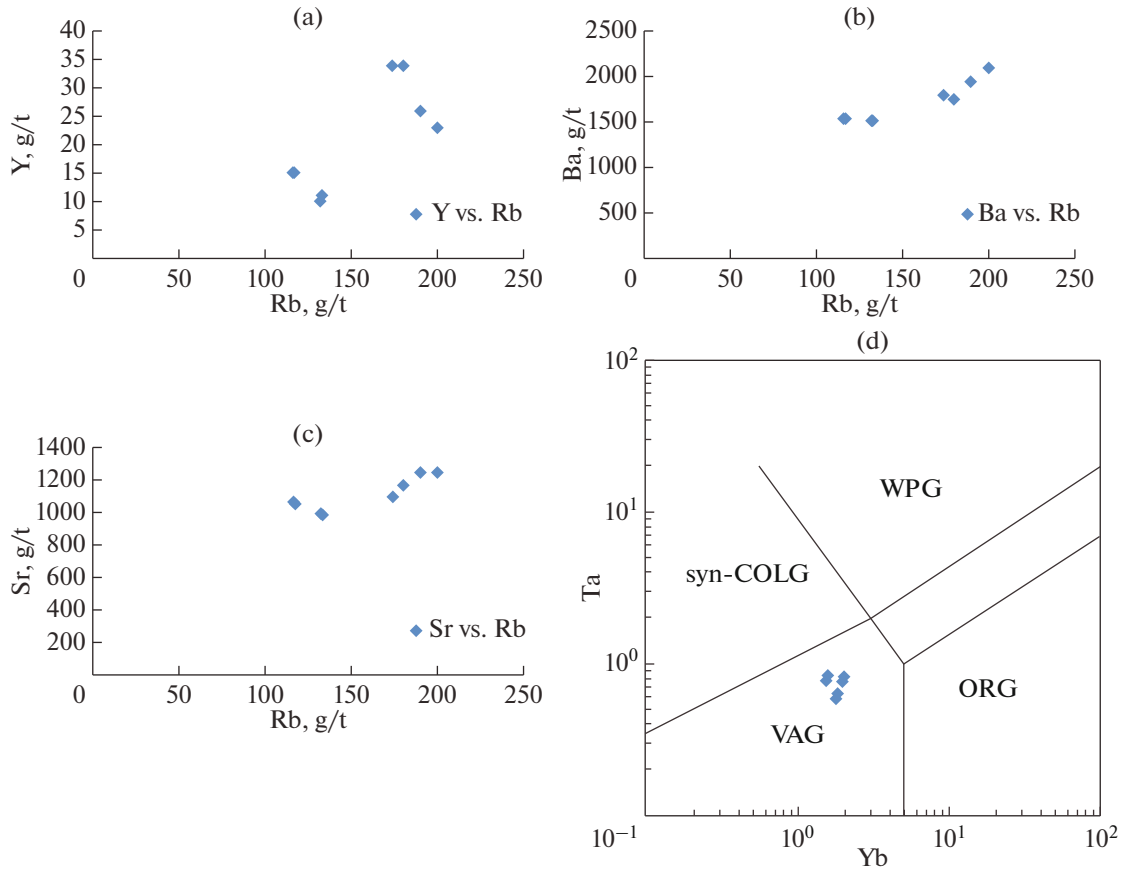


**Fig. 7.** Diagrams of Kozuf trachydacite–trachyandesites: (a) Y–Rb; (b) Ba–Rb; (c) Sr–Rb; (d) discrimination diagram (Pearce et al., 1984). WPG, within-plate granites; syn-COLG, syncollisional granites; VAG, volcanic arc, and orogen granites.

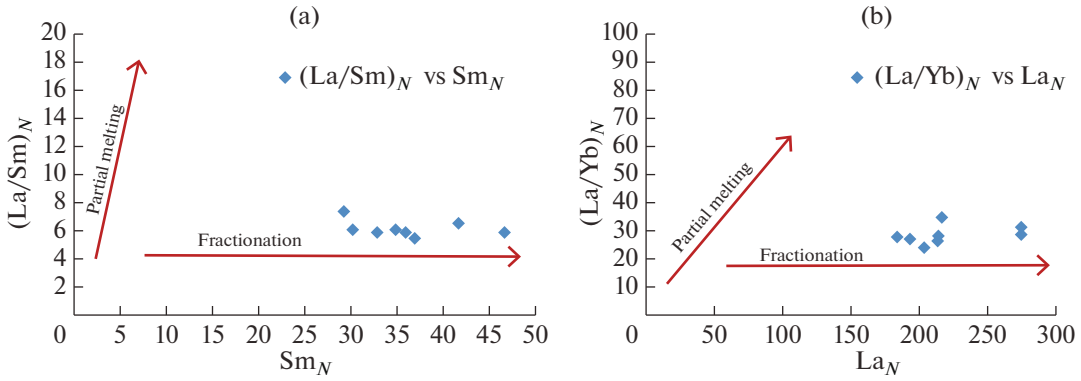


**Fig. 8.** Diagrams: (a) La/Sm–Sm; (b) La/Yb–La; Dudica deposit.

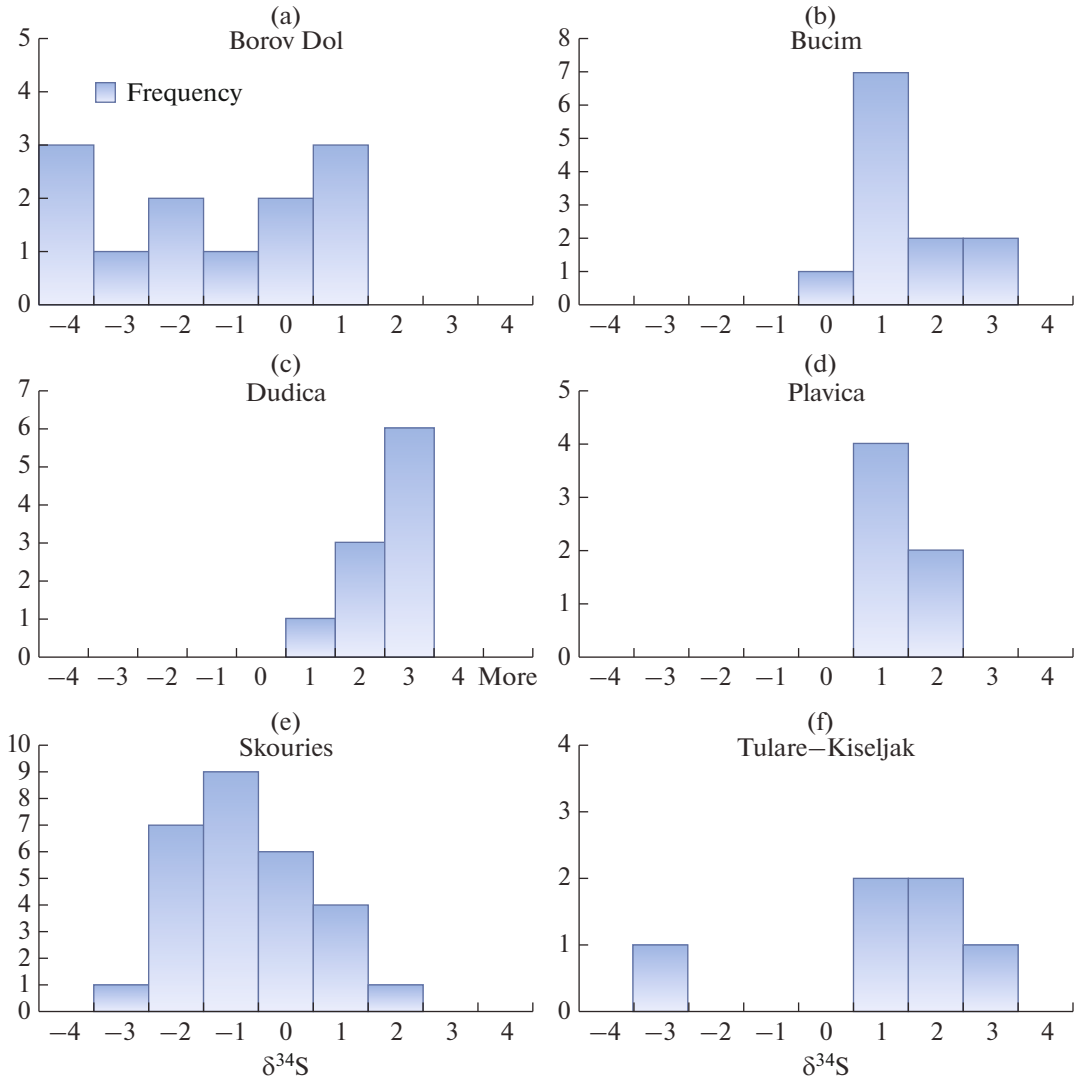


**Fig. 9.** $\delta^{34}S$ values of sulfides at Tulare–Kiseljak, Plavica, Bucim, Borov Dol, Dudica, and Skouries deposits.

Fig. 9). The $\delta^{34}S$ values most similar to those for the Dudica are from 0.00 to +2.50‰ for the Bucim deposit (Serafimovski, 1993; Serafimovski and Tasev, 2013b; Serafimovski et al., 2016) and from +0.41 to +1.24‰, for the Plavica deposit (Serafimovski, 1993). At the same time, $\delta^{34}S$ values for the Skouries deposit are in the interval from −3.20 to +1.28‰ (Serafimovski, 1993). The Tulare–Kiseljak and Borov Dol deposits are characterized by a slight widening of variation ranges toward the negative $\delta^{34}S$ values (Serafimovski, 1993), from −3.36 to +2.55‰ and from −4.05 to +0.72‰, respectively (Fig. 9). To summarize, the obtained spectrum of $\delta^{34}S$ values is similar to the spectrum characteristic of magmatic sulfur, $0 \pm 5$‰ (Ohmoto and Rye, 1979).

The established range of $\delta^{34}S$ values in sulfide minerals at the Dudica deposits is representative of ore mineralization in granitoid rocks and porphyry Cu ± Mo deposits (Douglas et al., 2003). The narrow range of $\delta^{34}S$ values for pyrite, chalcopyrite, galena, and enargite (from +1.0‰ to 2.5‰) suggests a relatively homogeneous sulfur source (Ohmoto and Rye, 1979; Hedenquist et al., 2017).

Data obtained at the end of last century, as well as our studies, indicate the complex structure of the Dudica deposit, which is most adequately comparable with the structure of the Plavica deposit (Serafimovskii et al., 2017), where the highest gold concentrations are associated with secondary quartzite bodies. Similar orebodies are widely developed in the high-sulfidation epithermal ore deposits worldwide (Sillitoe and Hedenquist, 2003; Richards, 2009). Mineralization similar to the Dudica was discovered in the Tulare deposit in Serbia (Janković, 1997), where it transforms into porphyry copper mineralization at deeper levels. In addition, similar ore manifestations were encountered in the Petrosnica orefield near Kumanovo, the Republic of North Macedonia (M'nkov et al., 2015).

The occurrence of alunitization along with secondary quartzites, porous quartz, native sulfur bodies, and the argillic alteration type evidence the development of high-sulfidation epithermal mineralization (enargite, pyrite, and gold) in the Dudica orefield (Sillitoe and Hedenquist, 2003).

## FUNDING

This study was supported by the State Task for the Institute of Geology of Ore Deposits, Petrography, Mineralogy, and Geochemistry, Russian Academy of Sciences (project no. AAAA-A18-118021590164-0).

## CONFLICT OF INTEREST

The authors declare that they have no conflict of interest.

## REFERENCES

Bau, M., Rare-earth element mobility during hydrothermal and metamorphic fluid-rock interaction and the significance of the oxidation state of europium, *Chem. Geol.,* 1991, vol. 93, nos. 3–4, pp. 219–230.

Boev, B., Petrological, Geochemical, and Volcanic Features of Volcanic Rocks of the Kozuf Mountain, *Doctoral Thesis,* Stip: University St. Cyril and Methodius, 1988.

Boev, B. and Yanev, Y., Tertiary magmatism within the Republic of Macedonia: a review, *Acta Vulcanologica,* 2001, vol. 13, nos. 1–2, pp. 57–71.

Boev, B. and Jelenkovic, R., Allchar deposit in Republic of Macedonia. petrology and age determination, *Petrology—New Persp. Appl.,* 2012, vol. 64, pp. 132–168.

Bogojevski, K., *Gold in Macedonia: Geology, Metallogenic Features, Ore Occurrences, Gold Ore Deposits and their Evaluation*, Skopje: University "St. Cyril and Methodius", 1998.

Boynton, W.V., *Geochemistry of the rare earth elements: meteorite studies, Rare Earth Element Geochemistry,* Henderson, P., Ed., Oxford: Elsevier, 1984, pp. 63–114.

Carmichael, I.S.E. and Ghiorso, M.S., The effect of oxygen fugacity on the redox state of natural liquids and their crystallizing phases, *Rev Mineral,* 1990, vol. 24, pp. 191–212.

Chen, B., Long, X., Wilde, A.S., et al., Delamination of lithospheric mantle evidenced by Cenozoic potassic rocks in Yunnan, SW China: a contribution to uplift of the Eastern Tibetan plateau, *Lithos,* 2017, vol. 284–285, pp. 709–729.

Dimitrijevic, M., *The Serbo-Macedonian massif, Tectonic of the Carpathian-Balkan Regions.* Bratislava: Geological Institute of Dyoniz Stura, 1974, pp. 291–296.

Douglas, T.A., Chamberlain, C.P., Poage, M.A., et al., Fluid flow and the heart mountain fault: a stable isotopic, fluid inclusion, and geochronologic study, *Geofluids,* 2003, vol. 3, pp. 13–32.

Hanson, G.N., Rare earth elements in petrogenetic studies of igneous systems, *Annu. Rev. Earth Planet. Sci.,* 1980, vol. 8, pp. 371–406.

Hedenquist, W.J., Arribas, R.A., and Aoki, M., Zonation of sulfate and sulfide minerals and isotopic composition in the Far Southeast porphyry and Lepanto epithermal Cu–Au deposits, Philippines, *Resour. Geol.,* 2017, vol. 67, pp. 174–196.

Hiessleitner, G., Das enargitvorkommen dudice in mazedonien, *Geol. Bundesanst.,* 1945, vol. 1, pp. 53–93.

Ivanov, T., Metallogeny of the Southern Part of the Vardar Zone, *Doctoral Thesis,* Belgrade: Faculty of Mining and Geology, 1965.

Janković, S., *Deposits of Metallic Mineral Resources,* Belgrade: Faculty of Mining and Geology, 1967.

Janković, S., The Carpatho–Balkanides and adjacent area: a sector of the Tethyan Eurasian metallogenic belt, *Miner. Deposita,* 1997, vol. 32, pp. 426–433.

Jankovic, S., Boev, B., and Serafimovski, T., *Magmatism and Tertiary Mineralization of the Kozuf Metallogenetic District, the Republic of Macedonia with Particular Reference to the Alsar Deposit,* Skopje: University "Sts. Cyril and Methodius", 1997.

Karamata, S., Plate tectonic phenomena in the regions of the Tethys type, *Geotectonics,* 1984, vol. 17, pp. 52–66.

Kochneva, N.T., Volkov, A.V., Serafimovskii, T., Tasev, G., and Tomson, I.N., Tectonic position of the Alshar Au–As–Sb–Tl deposit, Macedonia, *Dokl. Earth Sci.,* 2006, vol. 407, no. 2, pp. 175–178.

Kolb, M., Von Quadt, A., Peytcheva, I., et al., Adakite-like and normal arc magmas: distinct fractionation paths in the East Serbian segment of the Balkan–Carpathian arc, *J. Petrol.,* 2013, vol. 54, no. 3, pp. 421–451.

LeMaitre, R.W., Bateman, P., Dudek, A., et al., *A Classification of Igneous Rocks and Glossary of Terms,* Oxford: Blackwell Scientific Publishers, 1989.

Lippolt, H.J. and Fuhrmann, U., K-Ar age determination on volcanics of Alsar mine/Yugoslavia, *Workshop on the Fasibility of Solar Neutrino Detection with $^{206}$Pb by Geochemical and Mass Spectroscopical Measurements*, Nolte, E., Eds., Munchen: Technische Univer, 1986, Report GSI-86-9.

M'nkov, Sl., Antonov, M., Siroshtan, D., et al., *Report for the Geological Mapping and Geophysical Studies of the Territory of the Concession Area Petroshnitsa, Republic of Macedonia-Project 2015*, Sofia: Geomac-Ltd, 2015.

Marchev, P., Kaiser-Rohrmeier, M., Heinrich, C., et al., Hydrothermal ore deposits related to post-orogenic extensional magmatism and core complex formation: the Rhodope massif of Bulgaria and Greece, *Ore Geol. Rev.,* 2005, vol. 27, pp. 53–89.

McLennan, S.M., Rare earth elements in sedimentary rocks: influences of provenance and sedimentary processes, *Rev. Mineral. Geochem.,* 1989, vol. 21, pp. 169–200.

Middlemost, E.A.K., Naming materials in the magma/igneous rock system, *Earth-Sci. Rev.,* 1994, vol. 37, nos. 3–4, pp. 215–224.

Moore, G. and Carmichael, I.S.E., The hydrous phase equilibria (to 3 kbar) of an andesite and basaltic andesite from Western Mexico: constraints on water content and conditions of phenocryst growth, *Contrib. Mineral. Petrol.,* 1998, vol. 130, pp. 304–319.

Müller, D., Rock, N.M.S., and Grooves, D.I., Geochemical discrimination between shoshonitic and potassic volcanic rocks in different tectonic settings: a pilot study, *Mineral. Petrol.,* 1992, vol. 46, pp. 259–289.

Najime, T., Abaa, S.I., and Magaji, S., Petrology and rare earth elements (REE) distribution patterns of magmatic rocks in Gboko Area, Lower Benue trough, Nigeria: implication for tectonic evolution, *Global J. Geol. Sci.,* 2012, vol. 10, pp. 47–58.

Ohmoto, H. and Rye, R.O., *Isotopes of sulfur and carbon, Geochemistry of Hydrothermal Ore Deposits,* Barnes, H.L., Eds., 2nd ed., New York: John Wiley, 1979.

Pearce, J.A., Harris, N.B.W., and Tindle, A.G., Trace element discrimination diagrams for the tectonic interpretation of granitic rocks, *J. Petrol.,* 1984, vol. 25, pp. 956–983.

Richards, J.P., Post-subduction porphyry Cu–Au and epithermal au deposits: products of remelting of subduction-modified lithosphere, *Geology,* 2009, vol. 37, pp. 247–250.

Serafimovski, T., *Structural Metallogenetic Characteristics of the Lece-Chakidiki Zone: Types of Mineral Deposits and Distribution*, Stip: Special Edition, 1993.

Serafimovski, T. and Tasev, G., Metallogeny of the Kozuf ore district, R. Macedonia, *Ist International Workshop on The Project Enigma, Proceedings Book,* Serafimovski, T., and Boev, B., Eds., 2013a, pp. 11–22.

Serafimovski, T. and Tasev, G., Sulfur isotope compositions from different type of deposits in the Buchim–Damjan–Borov Dol ore district, Eastern Macedonia, *10th Applied Isotope Geochemistry Conference, Hungarian Academy of Sciences, Budapest, Hungary,* 2013b, Budapest, pp. 8–13.

Serafimovski, T., Tasev, G., Srmic-Palinkas, S., et al., Porphyry Cu mineralization related to the small Tertiary volcanic intrusions in the Bucim ore deposit, eastern Macedonia, *Geol. Croatica,* 2016, vol. 69, pp. 103–121.

Serafimovski, T., Volkov, A.V., Boev B., and Tasev, G. Ržanovo metamorphosed lateritic Fe–Ni deposit, Republic of Macedonia, *Geol. Ore Deposits,* 2013, vol. 55, no. 5, pp. 383–398.

Serafimovski, T., Volkov, A.V., Serafimovski, D., Tasev, G, Ivanovski, I. and Murashov, K.Yu., Plavica eithermal Au–Ag–Cu deposit in Eastern Macedonia: geology and 3D model of valuable component distribution in ore, *Geol. Ore Deposits,* 2017, vol. 59, no. 4, pp. 296–304.

Sillitoe, H.R. and Hedenquist, W.J., Linkages between volcanotectonic settings, ore-fluid compositions, and epithermal precious metal deposits, *Soc. Econ. Geol. Sp. Publ,* 2003, vol. 10, pp. 315–343.

Volkov, A.V., Serafimovski, T., Kochneva, N.T., Tomson, I.N., and Tasev, G., The Alshar Epithermal Au–As–Sb–Tl Deposit, Southern Macedonia, *Geol. Ore Deposits*, 2006, vol. 48, no. 3, pp. 175–192.

*Translated by E. Murashova*